Journal of the Civil Engineering Forum
jurnal.ugm.ac.id/v3/jcef

VOLUME 13, ISSUE 1
January 2027, 13(1)
DOI: 10.22146/jcef.26693

RESEARCH ARTICLE

Estimation of Shear Wave Velocity to a Depth of 30 Meters Using the Monte Carlo HVSR Inversion Method on the North Coast of Bengkulu, Indonesia

Gita Panny Nababan[1], Budi Harlianto[1*], Refrizon[1], Darmawan Ikhlas Fadli[1,2], Erlan Sumanjaya[3], Muhammad Arib Alwansyah[4]

[1]Geophysics Study Program, University of Bengkulu, Muara Bangka Hulu, Bengkulu, INDONESIA
[2]Supply Chain Division, TBU PT OKI Pulp & Paper Mills, APP Sinarmas Group, Basuki Rahmat, Palembang, INDONESIA
[3]Department of Geodesy and Geomatics Engineering, University of Lampung, Bandar Lampung, INDONESIA
[4]Mathematics Education Department, Universitas Negeri Jakarta, East Jakarta, INDONESIA

ARTICLE HISTORY
Received: 14 December 2025
Revised: 18 April 2026
Accepted: 15 March 2026

CORRESPONDENCE
b.harlianto@unib.ac.id

ARTICLE DOI
10.22146/jcef.26693

KEYWORDS
Earthquake amplification; HVSR, microtremor; Monte Carlo inversion; V_{s30}

Abstract

Assessing seismic site conditions using the time-averaged shear-wave velocity of the upper 30 m (V_{s30}) is fundamental for understanding local site response and supporting seismic microzonation. This study investigates subsurface characteristics in the Ketahun region, North Bengkulu, by integrating the Horizontal-to-Vertical Spectral Ratio (HVSR) method with Monte Carlo inversion to obtain site-specific V_{s30} estimates that are physically consistent with observed spectral characteristics, rather than representing unique subsurface models. A total of 29 microtremor measurement stations were deployed using three-component seismometers, and microtremor data were processed with Geopsy to derive the dominant frequency (f_0) and site amplification factor (A_0). These parameters were used as input constraints in the inversion procedure to construct shear-wave velocity profiles. The inversion results yield V_{s30} values ranging from 257 to 1,220 m/s, indicating substantial lateral heterogeneity driven by variations in sediment thickness and bedrock depth. Lower V_{s30} values characterize coastal alluvial deposits, whereas higher values are associated with the eastern–northern hilly terrain dominated by shallow bedrock. A comparative assessment with the global USGS topographic-slope-based V_{s30} model reveals systematic discrepancies, with the USGS proxy consistently underestimating V_{s30} in hard-rock domains. Statistical analysis confirms that the differences between the two datasets are significant, indicating that slope-based proxies may not fully capture local subsurface variability in geologically complex environments. While HVSR inversion is inherently non-unique and is not constrained by independent boreholes or surface-wave data, the results provide a physically consistent representation of spatial variations in near-surface stiffness. These findings contribute to an improved understanding of site-condition variability in North Bengkulu and provide a useful basis for future integration with complementary geophysical or geotechnical investigations.

© The Author(s) 2027. This article is distributed under a Creative Commons Attribution-ShareAlike 4.0 International license.

1 INTRODUCTION

The phenomena of erosion, landslides, and seismic activity represent fundamental geodynamic processes that frequently occur throughout Indonesia. This condition is primarily attributed to the nation's tectonic setting at the convergence of the Indo-Australian, Eurasian, and Pacific plates (Hadi et al., 2025). One region strongly influenced by this tectonic interaction is the Ketahun Segment, situated between the Musi and Siulak Segments. Although the segment has exhibited relatively low seismicity in recent decades, historical records document two significant earthquakes such as *Ms* 7.3 in 1943 and *Ms* 6.8 in 1952 (Lubis et al., 2025; Sieh and Natawidjaja, 2000; Hurukawa et al., 2014), indicating that substantial seismic potential remains.

The Ketahun Segment lies within a hilly terrain where survey orientations generally parallel the principal fault trend. The contact zone between displaced blocks shows complex geological conditions, necessitating analytical approaches aligned with the structural framework (Myers and Aydin, 2004; Hadi et al., 2025). To achieve a more comprehensive assessment of the segment's seismic characteristics, shear-wave velocity analysis is required. Given the geological heterogeneity and potential seismic activity, dynamic soil parameters particularly the average shear-wave velocity to 30 m depth (V_{s30}) serve as essential indicators of subsurface stiffness and seismic vulnerability. Shear-wave velocity is considered one of the most critical soil parameters because of its significant influence on site response analysis (Boore & Joyner, 1997, as cited in Akter, 2022). Near-surface shear-wave velocity is a critical parameter in for evaluating site response. V_{s30} is widely adopted in earthquake-resistant design codes and contributes substantially to seismic risk mitigation strategies (Yilmaz et al., 2024, as cited in Susilo et al., 2024). It for *Ms* a fundamental basis for dynamic soil classification and is incorporated into major seismic provisions such as Eurocode 8 and NEHRP (Castellaro and Mulargia, 2009). Moreover, V_{s30} is integral to seismic microzonation, as it reflects soil stiffness, potential ground-motion amplification, and sediment stability under dynamic loading (Simanjuntak et al., 2021; Hasaniyah et al., 2025).

In this study, the Horizontal-to-Vertical Spectral Ratio (HVSR) method is employed to derive shear-wave velocity estimates based on natural microtremor signals. These microtremors originate from atmospheric interactions and anthropogenic

sources, producing low-frequency ground motions detectable across broad geographic areas (Zaenudin et al., 2024). HVSR-based site characterization provides key parameters, including the predominant frequency (f_0), amplification factor (A_0), and shear-wave velocity (V_s) that collectively describe a site's dynamic response to seismic excitation (Zaenudin et al., 2024).

Despite the extensive application of HVSR in microzonation and dynamic site analysis, its use for V_{s30} estimation in regions with high lithological heterogeneity such as the Ketahun Segment remains limited. To date, no study has comprehensively integrated HVSR with Monte Carlo inversion to obtain representative V_{s30} models, nor quantitatively compared these models with topographic-slope-based V_{s30} estimates such as those developed by the USGS.

The global V_{s30} model developed by the United States Geological Survey (USGS) employs topographic slope as a proxy to estimate near-surface shear-wave velocity conditions. This approach is based on an empirical relationship whereby steep topography is generally associated with shallow bedrock and mechanically stiffer materials, whereas low-relief areas tend to be underlain by thicker and softer sedimentary deposits (Allen and Wald, 2007; 2009). Consequently, slope gradient has been widely adopted as an indirect parameter for mapping regional to global variations in V_{s30}, particularly in areas where in-situgeotechnical and geophysical data are sparse.

However, this assumption does not necessarily hold in tropical regions with complex tectonic settings, such as Indonesia. On Sumatra Island, the relationship between topographic slope and subsurface stiffness is often non-linear due to intense tropical weathering, the presence of thick residual soil layers, alteration of volcanic and Tertiary sedimentary rocks, and the influence of ongoing tectonic deformation. These conditions may result in relatively low V_{s30} values even in morphologically steep terrains. As a consequence, slope-based approaches may oversimplify local geological heterogeneity and lead to V_{s30} estimates that do not fully represent actual subsurface conditions, as has been documented in regions characterized by high geological complexity (Heath et al., 2020).

The absence of such integrative analyses introduces uncertainties in site classification and amplification estimation, thereby affecting the reliability of seismic hazard assessments and mitigation planning. Accordingly, this study aims to estimate V_{s30} through Monte Carlo inversion of HVSR curves derived from microtremor measurements and to compare the results with USGS slope-based V_{s30} values using p-value statistical evaluation. This study applies a Monte Carlo-based HVSR inversion method to derive site-specific V_{s30} values for the Ketahun Segment and presents the first statistically validated evaluation of the USGS topographic-slope-based V_{s30} model in North Bengkulu. The results indicate that HVSR-derived V_{s30} estimates provide a more reliable representation of subsurface conditions in regions characterized by high geological complexity.

2 METHODS

The methodology of this study is designed to quantitatively characterize the dynamic soil properties of the Ketahun region through an integrated approach combining microtremor analysis and HVSR inversion. The HVSR method is widely applied in seismic microzonation due to its non-destructive nature, cost-effectiveness, and capability to identify local resonance and estimate the depth of the bedrock interface (García-Jerez et al., 2016; Parolai et al., 2002). To obtain a more reliable shear-wave velocity model (V_s profile) and V_{s30} estimation, a Monte Carlo inversion approach is employed, allowing the incorporation of geological variability and inherent uncertainties in the subsurface structure.

2.1 Study Area and Data

The field investigation was conducted in the northern coastal area of Ketahun, North Bengkulu Regency, Bengkulu Province. This region was selected due to its complex geological setting and seismic potential associated with the Ketahun Fault, which forms part of the structural system linked to the Musi Fault (Figure 1).

Two types of data were utilized: primary and secondary datasets. Primary data were acquired through field surveys and direct microtremor measurements at 29 observation points. Measurements were performed using a three-component PASI Gemini-2 seismometer with a 2 Hz sensor response for the NS, EW, and vertical (Z) components (Fatimah et al., 2022). Data acquisition was focused on areas affected by the 1952 earthquake, with a recording duration of 30 minutes and a sampling frequency of 200 Hz, following SESAME guidelines.

Secondary data consisted of regional geological and seismological information to support the interpretation of field results, including the distribution of active faults, Peak Ground Acceleration (PGA) of bedrock, earthquake catalogs, slope gradients, rainfall data, shear-wave velocity profiles, V_{s30} values, and topographic maps. Additionally, the USGS V_{s30} model derived from the topographic slope method (Allen and Wald, 2007; 2009) was used for comparison. Comparative analysis involved evaluating differences in V_{s30} values, spatial patterns, and soil classification between HVSR inversion results and the USGS model. This dual approach enhances the reliability of subsurface interpretation by avoiding dependence on a single estimation method.

2.2 HVSR (Horizontal to Vertical Spectral Ratio)

The HVSR approach is widely used to estimate the depth of bedrock and evaluate subsurface resonance characteristics (Kencoro et al., 2023). It is widely recognized for its simplicity, non-destructive nature, low cost, and suitability for investigations in urban areas (Fatimah et al., 2022).

This method is particularly effective for determining the dominant frequency (f_0) and site amplification factor (A_0) (Harlianto et al., 2024). The HVSR technique enables the identification of local resonance characteristics and the detection of impedance contrasts between sedimentary layers and the underlying bedrock (Zaenudin et al., 2024). The HVSR ratio is generally calculated using the following expression (Equation 1):

$$\mathrm{H/V} = \sqrt{\frac{H^2(\mathrm{EW}) + H^2(\mathrm{NS})}{2V^2}} \tag{1}$$

where $H(\mathrm{EW})$ and $H(\mathrm{NS})$ denote the horizontal Fourier amplitude spectra in the east-west and north-south directions, respectively, and V represents the vertical Fourier amplitude

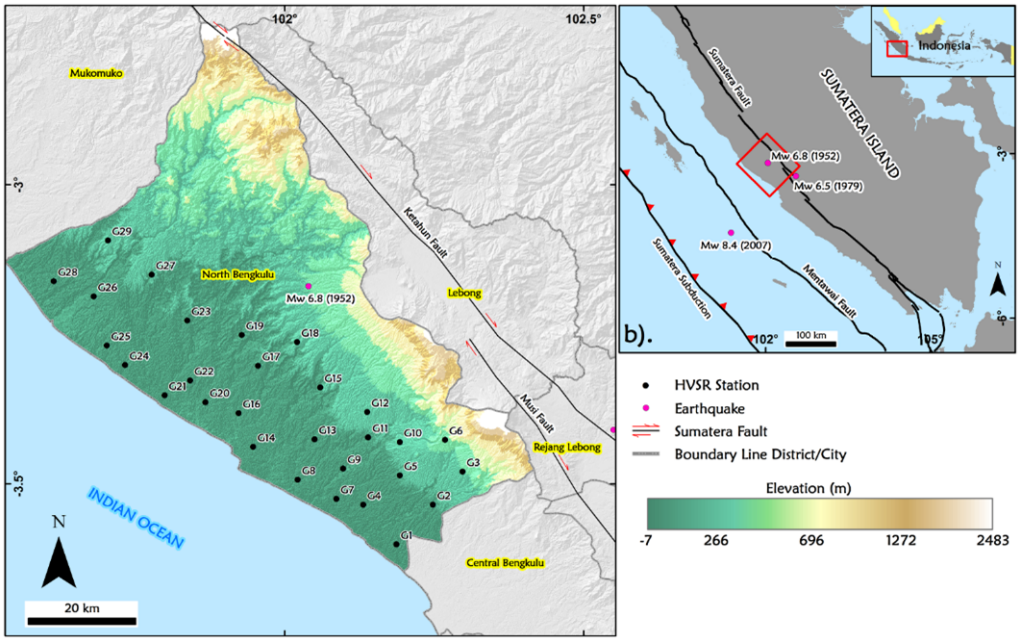


Figure 1. Topographic map of the study area showing the locations of microtremor measurement points.

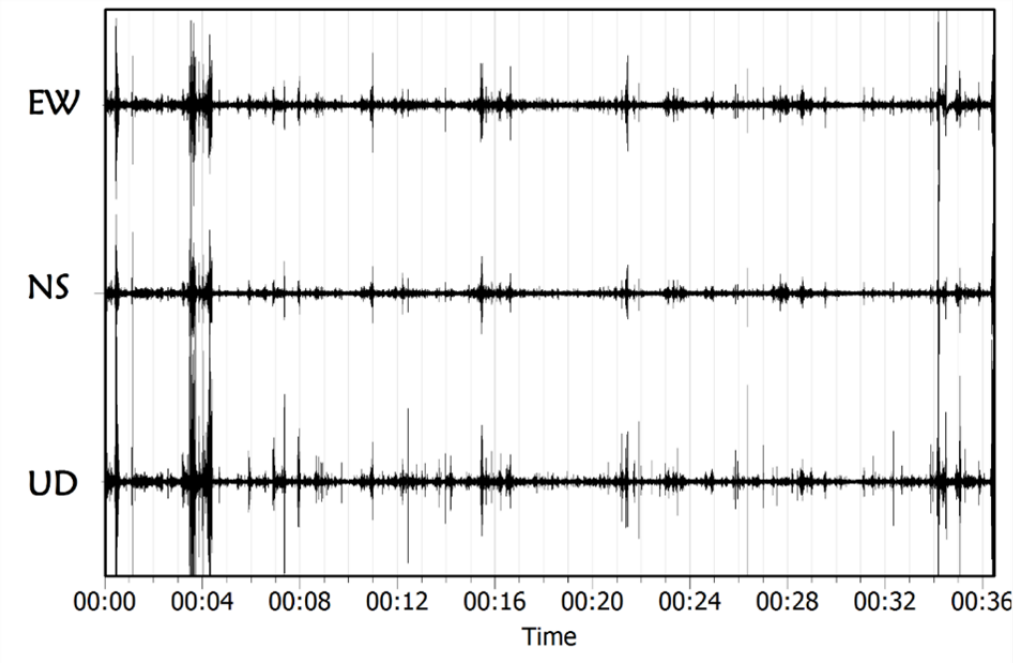


Figure 2. Example of three-component microtremor recordings (EW, NS, and UD) obtained during a 30-minute measurement period.

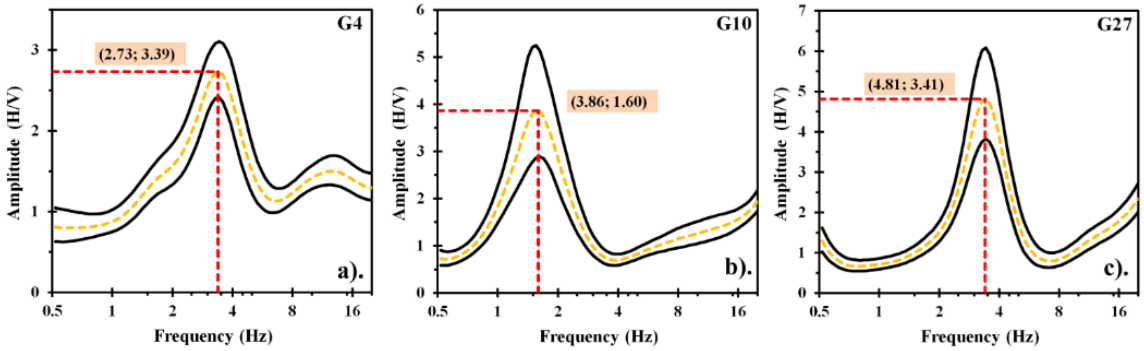


Figure 3. Example of an HVSR curve derived from microtremor data using Geopsy, showing the dominant frequency (f_0) and peak amplitude (A_0) at the observation site. The black lines represent the minimum and maximum H/V values, while the yellow dashed line indicates the average H/V curve.

spectrum (Mase et al., 2021). This ratio is used to identify the resonance peak corresponding to the natural frequency of the sedimentary layers.

Konno–Ohmachi smoothing with a coefficient of 20 was applied to reduce modulation effects and extreme spectral fluctuations. Quality control procedures followed SESAME criteria, including: (1) minimum recording duration of 2030 minutes; (2) segmentation of records into windows of 2040 seconds; (3) exclusion of transient noise such as traffic or wind; (4) ensuring a consistent peak with amplitude coefficient of variation (CV) < 0.3; (5) stability checks across windows; and (6) validity of the curve only when one clear resonance peak is observed.

HVSR analysis was performed using Geopsy software developed during the SESAME project (Wathelet et al., 2020). The dataset was recorded in SAF format and processed using the H/V module to extract H/V ratios, dominant frequencies, and peak amplitudes. Theoretically, when microtremor signals are dominated by fundamental Rayleigh waves, the HVSR curve exhibits a sharp resonance peak corresponding to the depth of the bedrock. However, real-world conditions often involve additional vertical components that may reduce peak amplitudes (Stephenson, 2007). Therefore, the interpretation must ensure peak stability and reliability for accurate subsurface characterization.

2.3 Monte Carlo Inversion

After the HVSR parameters had been obtained, the next step was to perform the inversion process to derive the subsurface shear-wave velocity profile (V_s profile) and the corresponding V_{s30} values. This process was carried out using a Monte Carlo inversion method, as described by García-Jerez et al. (2016). The approach employs the Metropolis sampling algorithm (Metropolis et al., 1953) to explore the probability distribution of subsurface models that are consistent with the observed HVSR curves. The parameter space is sampled in a random yet controlled manner, yielding an ensemble of models that represent the variability of the physical properties of soil and rock layers. Within this framework, each model is evaluated based on the level of agreement between the theoretically calculated HVSR curve and the observed HVSR curve. Consequently, the inversion does not rely on a single optimal solution but rather on a set of physically acceptable solutions. The Monte Carlo inversion approach was selected because it effectively accommodates subsurface parameter uncertainty and local geological heterogeneity, which are often difficult to capture using simple deterministic inversion methods.

In this study, the subsurface model is assumed to consist of three sedimentary layers overlying an elastic half-space, a configuration commonly adopted for Quaternary sedimentary environments with relatively shallow bedrock (García-Jerez et al., 2016; Foti et al., 2018). Each layer is characterized by key physical parameters, including layer thickness, P-wave velocity (V_p), S-wave velocity (V_s), density, and Poissons ratio (Table 1). The minimum and maximum values assigned to these parameters were treated as prior constraints in the inversion scheme, allowing the Monte Carlo process to explore a broad parameter space while maintaining physically and geologically reasonable models. These bounds define the search space used by the Geopsy Monte Carlo inversion algorithm.

In this study, the subsurface was parameterized using a fixed-layer model consisting of three sedimentary layers overlying an elastic half-space. This configuration was selected a priori based on the general geological setting of the study area, which is characterized by Quaternary sedimentary deposits underlain by relatively shallow bedrock. The use of a fixed number of layers is a common practice in HVSR inversion studies to reduce model ambiguity and ensure inversion stability, particularly in the absence of complementary constraints such as borehole data or surface-wave dispersion measurements (García-Jerez et al., 2016; Foti et al., 2018). Subsurface variability was therefore accommodated through broad search ranges for the physical parameters of each layer, rather than by varying the number of layers.

No direct subsurface constraints, such as borehole logs, Standard Penetration Test (SPT) data, or surface-wave dispersion curves, were available to explicitly define or validate the depth of the first layer in the inversion model. Consequently, there was no independent control on the depth of the uppermost interface, and its thickness was entirely determined within a wide but geologically reasonable search range, informed by the general stratigraphic characteristics of coastal and alluvial Quaternary deposits in the study area. As a result, the depth of the shallowest layer interface is associated with a relatively high degree of uncertainty. Such limitations in vertical resolution are a well-known characteristic of one-dimensional HVSR-based inversion when independent geotechnical or geophysical constraints are lacking (Bonnefoy-Claudet et al., 2006; García-Jerez et al., 2016; Foti et al., 2018). It is important to emphasize that this uncertainty primarily affects the precision of individual layer depth estimates in the V_s profiles, rather than the overall V_{s30} values. V_{s30}, defined as the average shear-wave velocity down to 30 m depth, is inherently less sensitive to uncertainties in the position of any single layer boundary (García-Jerez et al., 2016; Foti et al., 2018).

Although a Monte Carlo-based HVSR inversion approach was employed to estimate shear-wave velocity (V_s) profiles, it must be explicitly acknowledged that inversion of H/V curves alone is mathematically non-unique. An inherent trade-off exists between layer thickness and shear-wave velocity, whereby a shallow low-velocity layer may produce a dominant resonance frequency comparable to that of a deeper layer with higher velocity. Consequently, a single best-fit V_s profile derived from HVSR inversion cannot be regarded as a unique representation of the subsurface structure. This limitation has been widely documented in the literature and is intrinsic to one-dimensional HVSR inversion in the absence of independent constraints such as borehole information or surface-wave dispersion data (Bonnefoy-Claudet et al., 2006; García-Jerez et al., 2016; Foti et al., 2018).

To mitigate the impact of this non-uniqueness, the present study does not rely on a single optimal solution but instead considers the ensemble of models generated through the Monte Carlo inversion process. This probabilistic framework allows exploration of multiple combinations of layer thicknesses and velocities that are equally consistent with the observed HVSR curves. Accordingly, the interpretation does not focus on the exact depth of individual layer interfaces,

Table 1. Search space (minimum and maximum bounds) of inversion parameters used in the Monte Carlo HVSR inversion implemented in Geopsy.

Layer	Thickness (m)	V_p (m/s)	V_s (m/s)	Density (kg/m^3)	Poissons Ratio
First Layer	10-20	250-1500	100-760	1800-2000	0.2-0.4
Second Layer	10-20	250-1500	100-760	1800-2000	0.2-0.4
Third Layer	10-20	250-1500	100-760	1800-2000	0.2-0.4
Half-space	10-20	1500-2600	760-1500	2000-2200	0.1-0.3

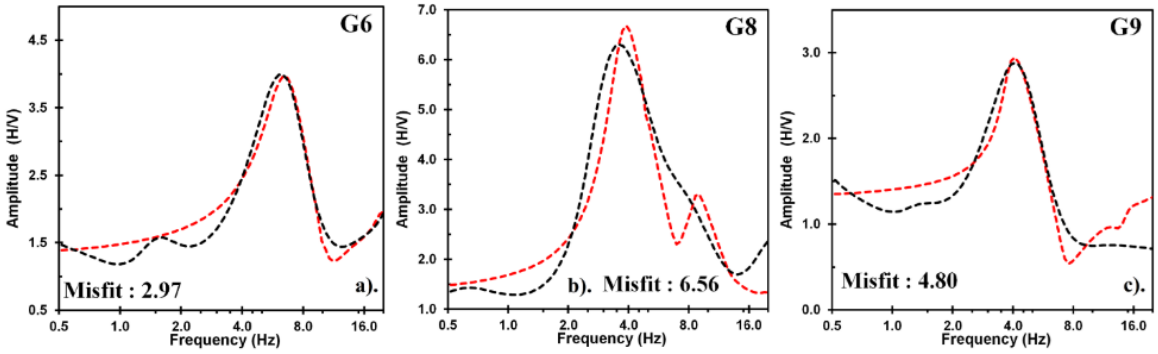


Figure 4. Example of observed and calculated H/V curves illustrating the misfit between the two datasets. The black dashed line represents the observed H/V curve, while the red dashed line indicates the calculated H/V curve obtained from the inversion model.

which are subject to substantial uncertainty, but rather on integrated parameters such as V_{s30}. As an averaged shear-wave velocity over the upper 30 m, V_{s30} is generally more robust with respect to thickness-velocity trade–offs than detailed layer geometries and thus provides a more stable metric for site characterization (García-Jerez et al., 2016; Foti et al., 2018).

2.4 Estimation of V_{s30} and Soil Classification

The average shear-wave velocity to a depth of 30 m (V_{s30}) was derived from the shear-wave velocity (V_s) profiles obtained through Monte Carlo inversion of the HVSR curves. Accordingly, the resulting V_{s30} values are not directly extracted from the raw HVSR curves but are computed from layered V_s models that physically represent subsurface conditions.

For each measurement site, a single V_{s30} value was determined as a representative parameter calculated from the inverted V_s model. This value reflects the average shear-wave velocity down to a depth of 30 m at each HVSR station and is used as a primary parameter for evaluating seismic site response within the study area.

Soil classification based on V_{s30} is of particular importance because it directly influences seismic wave amplification and site response and serves as a key parameter in earthquake-resistant design regulations and seismic hazard mapping (Allen and Wald, 2007; 2009). Therefore, the V_{s30} values obtained from the HVSR inversion were classified according to the NEHRP (National Earthquake Hazards Reduction Program) standard (Nugraheni et al., 2024; Harlianto et al., 2024) to identify variations in seismic site conditions across the measurement locations.

3 RESULTS AND DISCUSSION

HVSR analysis at 29 observation sites reveals dominant frequencies (f_0) ranging from 0.77 to 14.26 Hz, with a mean value of approximately 4.3 Hz. Most HVSR curves exhibit a distinct single peak, indicating a pronounced impedance contrast between overlying sediments and the underlying bedrock (Bonnefoy-Claudet et al., 2006). Sites with $f_0 < 2$ Hz, which are concentrated in the western part of the study area, reflect thick unconsolidated sedimentary deposits. Conversely, sites with $f_0 > 8$ Hz, primarily located in the eastern and northern sectors indicate shallow bedrock conditions. Representative curves (G6, G8, G9) in Figure 4 illustrate variability in amplitude and inversion misfit (misfit: 2.97, 6.56, 4.80), where lower misfit values denote better agreement between observed and modeled HVSR curves (García-Jerez et al., 2016).

Table 2. Soil classification is determined based on national seismic-resistance standards using V_{s30} criteria (Mase et al., 2021; Nugraheni et al., 2024).

Soil Classification	V_{s30} (m/s)
Hard Rock (A)	$V_{s30} \geq 1500$
Rock (B)	$760 < V_{s30} \leq 1500$
Very Dense Soil and Soft Rock (C)	$360 < V_{s30} \leq 760$
Stiff Soil (D)	$180 < V_{s30} \leq 360$
Soft Soil (E)	$V_{s30} < 180$

Based on the inversion of the HVSR curves, shear-wave velocity (V_s) profiles were derived for each measurement site. To represent model uncertainty arising from the inherent non-uniqueness of HVSR inversion, the resulting V_s profiles are not presented as a single best-fit solution only. Instead, an ensemble of accepted models within a defined misfit range is visualized to illustrate the range of solutions that are equally consistent with the observed HVSR curves. These accepted models are displayed as thin lines, while the model with the lowest misfit is highlighted as a thicker reference line. This approach is commonly adopted in HVSR-based inversion studies to explicitly illustrate model uncertainty and the variability of subsurface structures resulting from parameter trade-offs (García-Jerez et al., 2016; Foti et al., 2018).

In Figure 5, the shear-wave velocity (V_s) profiles are shown as a collection of Monte Carlo inversion models that satisfy the misfit acceptance criteria. All accepted models are plotted as thin lines to represent the range of physically plausible

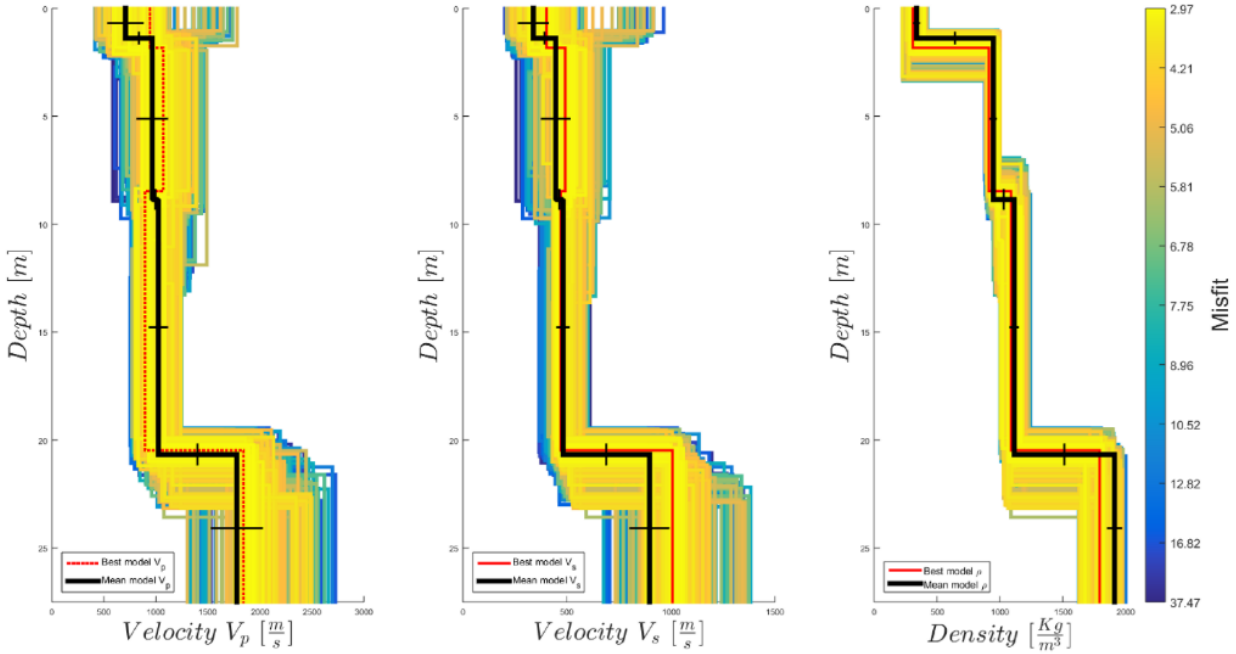


Figure 5. Example of shear-wave velocity (V_s) profiles obtained from Monte Carlo HVSR inversion. Thin lines represent the ensemble of accepted models satisfying the misfit criterion, illustrating model uncertainty. The bold line indicates the lowest-misfit model representing the best-fitting solution. The red dashed line represents the best model, while the black dashed line indicates the mean model of the accepted models.

subsurface solutions consistent with the observed HVSR response, whereas the lowest-misfit model is plotted as a bold line to indicate the best-fitting solution. This representation emphasizes the non-unique nature of HVSR inversion results, demonstrating that subsurface interpretation should not rely on a single deterministic V_s profile, but rather on the ensemble of acceptable solutions. By explicitly visualizing model uncertainty associated with inversion parameter trade-offs, this approach provides a more robust basis for assessing the reliability of the derived V_{s30} estimates.

The distribution of dominant frequency (f_0) values derived from the HVSR analysis exhibits strong spatial consistency with the pattern of V_{s30} variations obtained from the HVSR inversion, as shown in figure 6a. Coastal zones are characterized by relatively low V_{s30} values (<400 m/s), accompanied by low f_0 values, indicating the presence of thick, unconsolidated sediments and mechanically soft materials. In contrast, the hilly areas in the north eastern sector display high V_{s30} values (>900 m/s) together with elevated f_0 values, reflecting geological conditions dominated by shallow bedrock or more compact lithological units. This coherent pattern suggests that the lateral heterogeneity of V_{s30} in the Ketahun area is primarily controlled by the distribution of sedimentary facies and variations in bedrock depth.

In the context of evaluating inversion reliability, several measurement sites exhibit relatively higher inversion misfit values, which are mainly attributed to the local complexity of the HVSR curve shapes rather than to deficiencies in the inversion process itself. Sites with higher misfit values were therefore retained in the interpretation, as the V_{s30} estimates were derived from an ensemble of Monte Carlo-inverted models that remain physically acceptable. This ensemble-based approach allows the V_{s30} values to remain stable despite inter-model misfit variability. Consequently, relatively high misfit values do not directly reduce the reliability of the V_{s30} estimates but are instead interpreted as indicators of increased local uncertainty that should be considered in more detailed site-response analyses.

To achieve a more comprehensive interpretation of the V_{s30} distribution in Ketahun, the results of this study are placed within a regional context by comparison with previous microzonation studies conducted in Bengkulu City. These studies indicate that V_{s30} values in Bengkulu City generally fall within the range of medium to relatively stiff soils, which are predominantly classified as Site Class C in standard seismic site classifications. This condition has been attributed to the presence of denser subsurface materials and relatively shallow bedrock in parts of the urban area (Mase et al., 2021).

In contrast, the results from Ketahun reveal that most V_{s30} values are lower and more frequently correspond to soft to medium soil conditions (site class D to the lower bound of class C). This contrast suggests that subsurface conditions in Ketahun are dominated by thicker and less consolidated sedimentary layers compared to those underlying Bengkulu City. From a regional perspective, these findings indicate that soils in Ketahun are generally softer than those characterizing much of Bengkulu City. This difference in subsurface stiffness has direct implications for local seismic response. Lower V_{s30} values in Ketahun imply a higher potential for seismic wave amplification, suggesting that this area is likely to exhibit greater site response sensitivity relative to Bengkulu City, where subsurface conditions are predominantly characterized by stiffer soils.

The USGS V_{s30} map presented in Figure 6b shows a markedly more homogeneous spatial pattern and a narrower range of values compared to the HVSR inversion results, highlighting the need for a quantitative comparison between the two approaches.

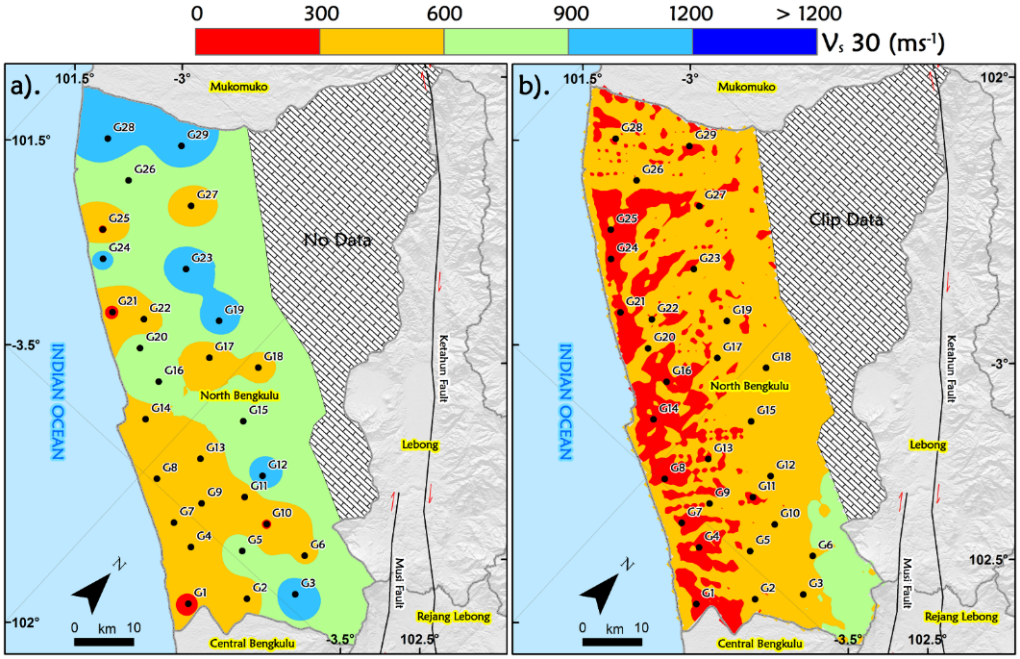


Figure 6. Comparison of V_{s30} maps derived from HVSR inversion and the USGS model. (a) V_{s30} map obtained from HVSR inversion. (b) V_{s30} map derived from the USGS global V_{s30} model, illustrating spatial differences between the two approaches.

A comparison between V_{s30} values derived from the HVSR inversion and those obtained from the USGS model was conducted to evaluate whether a global, topography-based approach can adequately represent actual subsurface conditions in a geologically heterogeneous region such as Ketahun. The HVSR inversion yields V_{s30} values controlled by local seismic response, particularly sediment thickness and bedrock depth, whereas the USGS V_{s30} estimates are indirectly inferred from topographic slope (Bonnefoy-Claudet et al., 2006; García-Jerez et al., 2016). By comparing the two datasets in terms of spatial patterns, site classification, and statistical characteristics, it is possible to assess whether the USGS model tends to underestimate or smooth subsurface stiffness variations. This comparison is critical because V_{s30} is a key parameter in site classification and seismic wave amplification estimation; therefore, inaccuracies in V_{s30} may directly affect seismic microzonation and earthquake hazard assessment.

Based on the V_{s30} values obtained from the HVSR inversion, soil classification according to the NEHRP (1998) standard, widely applied in contemporary seismic hazard studies (Mase et al., 2021; Nugraheni et al., 2024), is presented in Figure 7.

The V_{s30} values used to generate the soil classification map in Figure 7 were calculated from the V_s profiles obtained through HVSR inversion at each measurement station. To quantitatively illustrate the differences between the inversion results and the global USGS estimates, the V_{s30} values and corresponding site classifications for all measurement points are summarized in Table3.

Table3 shows that V_{s30} values derived from HVSR inversion span a substantially wider range (257-1220 m/s) than those estimated by the USGS model (215-549 m/s), indicating the ability of the inversion approach to more realistically capture variations in lithology and bedrock depth. The resulting differences in site classification, particularly in the eastern-northern hilly areas, further suggest that the USGS topographic-slope-

Table 3. V_{s30} values and site classification at each measurement point.

Site	V_{s30} Inv	Site Class	V_{s30} USGS	Site Class
G1	261,05	D	267,93	D
G2	504,36	C	341,97	C
G3	1203,41	B	464,12	C
G4	460,00	C	284,77	D
G5	771,39	B	341,56	D
G6	565,81	C	549,60	C
G7	323,10	D	273,80	D
G8	315,37	D	259,36	D
G9	558,06	C	307,90	D
G10	273,29	D	355,62	D
G11	281,59	D	292,43	D
G12	1220,35	B	363,17	C
G13	443,20	C	273,02	D
G14	580,98	C	261,02	D
G15	906,05	B	440,75	C
G16	682,97	C	277,16	D
G17	319,48	D	343,82	D
G18	544,52	C	414,15	C
G19	1129,72	B	333,76	D
G20	680,29	C	341,96	D
G21	257,40	D	287,66	D
G22	521,60	C	305,90	D
G23	1159,25	B	330,62	D
G24	1007,24	B	215,75	D
G25	278,96	D	292,06	D
G26	711,79	C	387,07	C
G27	405,64	C	269,75	D
G28	1120,77	B	323,00	D
G29	1098,15	B	283,64	D

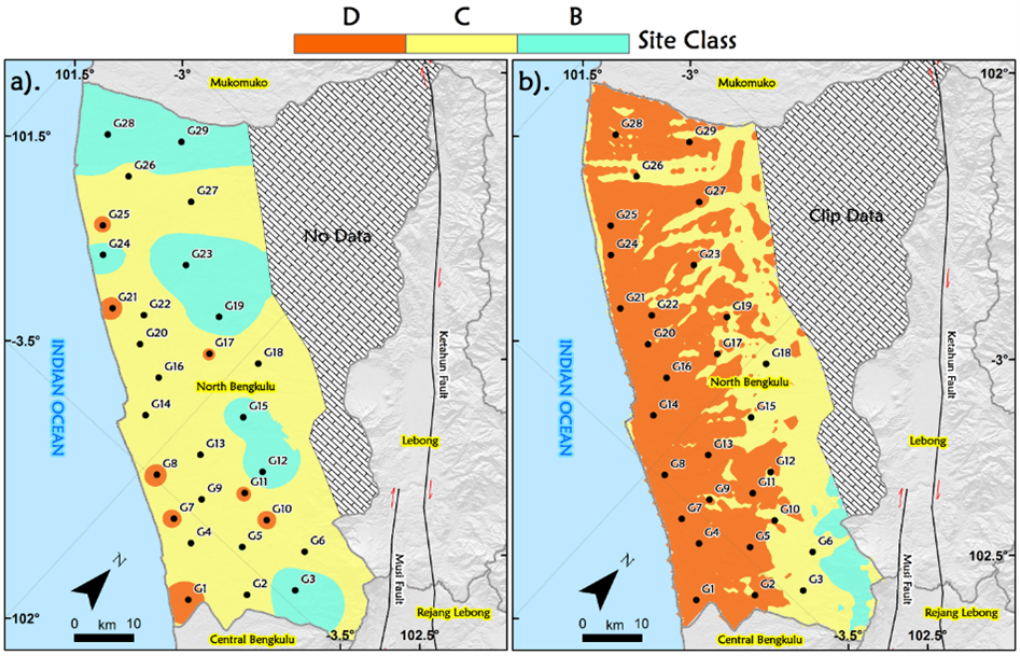


Figure 7. Soil classification based on V_{s30} values according to the NEHRP standard. (a) Soil classification derived from V_{s30} values obtained through HVSR inversion. (b) Soil classification based on V_{s30} values from the USGS model.

based approach tends to smooth local geological heterogeneity (Allen and Wald, 2007; 2009).

As illustrated in Figure 6, Class D soils (V_{s30} = 180-360 m/s) dominate the western sector and include sites G1, G7, G8, G10, G11, G17, G21, and G25. These low-velocity zones correspond to unconsolidated to semi-consolidated alluvial deposits, which generally exhibit higher seismic amplification potential. Class C soils (V_{s30} = 360-760 m/s) are distributed across the central to eastern regions and include sites G2, G4, G6, G9, G13, G14, G16, G18, G20, G22, G26, and G27. These values represent dense soils to soft rock and mark a transitional zone from alluvial sediments to more compact lithological units. Class B soils ($Vs_{30} > 760$ m/s) are observed at sites G3, G5, G12, G15, G19, G23, G24, G28, and G29, predominantly concentrated in the eastern-northern hilly domain. These sites correspond to shallow bedrock conditions characterized by high material stiffness and reduced amplification potential.

Geologically, the spatial variation of V_{s30} in the Ketahun area is controlled by differences in sedimentary facies and bedrock depth, as reflected in the regional topography (Figure 1). The coastal zone is dominated by young alluvial deposits consisting of loose sand, silt, and unconsolidated Quaternary materials formed through fluvial and marine-alluvial depositional processes. These fine-grained and poorly consolidated lithologies yield low V_{s30} values (< 400 m/s) and low dominant frequencies (f_0), reflecting significant sediment thickness. Such low f_0 conditions are commonly associated with high amplification factors (A_0), as seismic waves are amplified while propagating through thick, soft sediments.

In contrast, the eastern-northern hilly region is composed primarily of volcanic rocks and compacted Tertiary sediments with relatively shallow bedrock. These geological conditions produce high V_{s30} values (> 900 m/s), higher dominant frequencies, and lower amplification factors, as thin sediment cover and stiff lithologies reduce amplification potential. The observed correlation between increasing f_0 and decreasing sediment thickness in this area confirms that bedrock depth is a key factor controlling the lateral heterogeneity of dynamic soil properties across the study area.

To provide a geological interpretation of the observed V_{s30} variations, the relationship between shear-wave velocity and soil-rock material types follows follow the classification proposed by Foti et al. (2018) as summarized in Table4.

Table 4. Material type classification based on V_s values (Foti et al., 2018, as cited in Susilo et al., 2024).

Material	V_s **(m/s)**
Soft clay	80-200
Stiff clay	200-600
Loose sand	80-250
Dense sand	200-500
Gravel	300-900
Weathered rock	600-1000
Hard rock	1200-2500

Overall, these results indicate that the Ketahun area exhibits pronounced variability in site-class distribution, primarily controlled by changes in sediment thickness and variations in bedrock depth. Areas classified as Site Class D represent the most vulnerable zones with respect to seismic wave amplification, whereas Site Class B reflects relatively stable seismic conditions. Such spatial variability is critical for seismic microzonation planning, local hazard assessment, and the design of earthquake-resistant structures in the Ketahun region.

A comparison between V_{s30} values derived from HVSR inversion and those from the global USGS model reveals consistent differences across nearly the entire study area. The USGS approach, which is based on a topographic-slope proxy (Allen and Wald, 2007; 2009), tends to produce lower V_{s30} estimates within a relatively narrow range (approximately 215-

550 m/s). This behavior reflects the inherent characteristics of the method, which is more sensitive to surface slope than to actual subsurface conditions. This finding is consistent with the observations of Heath et al. (2020), who reported limitations of slope-based V_{s30} models in regions characterized by complex lithology or intense weathering.

In contrast, V_{s30} values obtained from the HVSR inversion span a much wider range (2571,220 m/s), reflecting lithological variability from alluvial sediments to shallow bedrock conditions. Spatially, both datasets show low V_{s30} values in the coastal zone; however, the most pronounced discrepancies occur in the eastern-northern hilly area. In this sector, the HVSR inversion indicates shallow bedrock with V_{s30} values exceeding 900 m/s, whereas the USGS model continues to classify the area as moderately stiff sediment (300-400 m/s). These discrepancies suggest that the USGS map is less capable of capturing the local geological heterogeneity of the Ketahun area and may therefore provide a less accurate representation of site conditions.

The statistically significant differences observed between V_{s30} values derived from HVSR inversion and those estimated by the USGS model highlight the limitations of topographic slope-based approaches in representing subsurface conditions in the Ketahun area. Global V_{s30} models such as those developed by the USGS rely on slope gradients derived from digital elevation models (DEMs), such as SRTM, as proxy parameters for estimating V_{s30}, based on an assumed empirical correlation between topographic slope and near-surface shear-wave velocity. However, several studies have demonstrated that this correlation is often weak or highly dependent on the length scale of the topographic metric employed, becoming more robust only when the metric captures large-scale relief rather than local slope gradients (Lin et al., 2019).

Other studies have further noted that the use of medium-resolution DEMs, such as SRTM, to compute slope-based V_{s30} proxies may lead to overly smoothed estimates in areas characterized by highly heterogeneous or variable topography. In such settings, fine-scale geomorphological variations are frequently not adequately captured by simple slope metrics (Allen and Wald, 2009). In the Ketahun region, complex lithological conditions, combined with spatial variability in sediment thickness and bedrock depth, give rise to subsurface dynamic responses that are not directly reflected by surface slope alone. Consequently, HVSR inversion results, which are grounded in local seismic response characteristics, tend to yield a more representative range of V_{s30} values than global topography-based proxy estimates. These findings indicate that the identified statistical differences are not merely numerical discrepancies but rather reflect the inherent limitations of topographic slope proxies when applied to regions with complex geological conditions.

The spatial differences observed between the V_{s30} maps derived from HVSR inversion and the USGS model (Figures 6 and 7) require quantitative evaluation to confirm that they represent physically meaningful contrasts rather than merely visual variations. Accordingly, descriptive analysis and statistical testing (t-test) were applied to the V_{s30} values obtained from the HVSR inversion (Figure 8a) and the USGS estimates (Figure 8b).

Descriptive analysis reveals a clear difference in the distribution of V_{s30} values derived from HVSR inversion and those estimated by the USGS model. The boxplot in Figure 8a shows that the HVSR-derived V_{s30} values span a much wider range (approximately 2571,220 m/s) and exhibit a higher median, reflecting the predominance of shallow bedrock conditions in the hilly areas. In contrast, the USGS-based V_{s30} values (Figure 8b) are confined to a relatively narrow interval (215-549 m/s), consistent with the tendency of the topographic-slope approach to produce more homogeneous estimates that are less sensitive to local lithological variability (Allen and Wald, 2009; Heath et al., 2020).

Visually, the boxplots indicate that the V_{s30} distribution obtained from HVSR inversion occupies a higher and more variable shear-wave velocity range compared to the USGS estimates, which are concentrated at lower values with relatively limited dispersion. This visual contrast provides an initial indication that the two methods yield non-equivalent V_{s30} estimates.

Statistical testing yields a t-value of 5.34 with 28 degrees of freedom and a p-value of 1.09×10^{-5}. Because the calculated t-value exceeds the critical t-value at the 5% significance level and the p-value is far below the threshold $\alpha = 0.05$, the null hypothesis (H_0) is rejected. This result indicates that the V_{s30} values derived from HVSR inversion and those estimated by the USGS model differ significantly. The mean difference of 313.88 m/s, with a confidence interval of 193.50-434.52 m/s, further demonstrates that this discrepancy is systematic rather than the result of random variability. The statistically significant difference between the two datasets suggests that the observed deviation is not attributable to measurement noise but instead reflects fundamental differences in how subsurface structures are represented, particularly in terms of bedrock depth and sediment-bedrock impedance contrasts.

Accordingly, these statistical results provide quantitative evidence that the application of the USGS topographic-slope-based V_{s30} model in the Ketahun area may lead to biased site classification and amplification estimates, potentially affecting the accuracy of seismic microzonation and earthquake-resistant design. This finding is consistent with (Allen and Wald, 2007), who highlighted the limitations of topography-based approaches in regions with complex geological structures. In contrast, the HVSR method combined with Monte Carlo inversion demonstrates greater sensitivity to impedance contrasts and sediment thickness (García-Jerez et al., 2016; Bonnefoy-Claudet et al., 2006), allowing for a more representative estimation of V_{s30}.

The statistically significant differences between V_{s30} values derived from HVSR inversion and those estimated by the USGS model indicate inherent limitations of topographic slope-based approaches in representing subsurface conditions in the Ketahun area. Global V_{s30} models, such as those developed by the USGS, employ surface slope as a proxy for soil stiffness based on empirical correlations established primarily from regions with relatively dense geotechnical data coverage (Allen and Wald, 2007; 2009). However, this approach is inherently indirect and does not explicitly incorporate information on local lithology, sediment thickness, or bedrock depth.

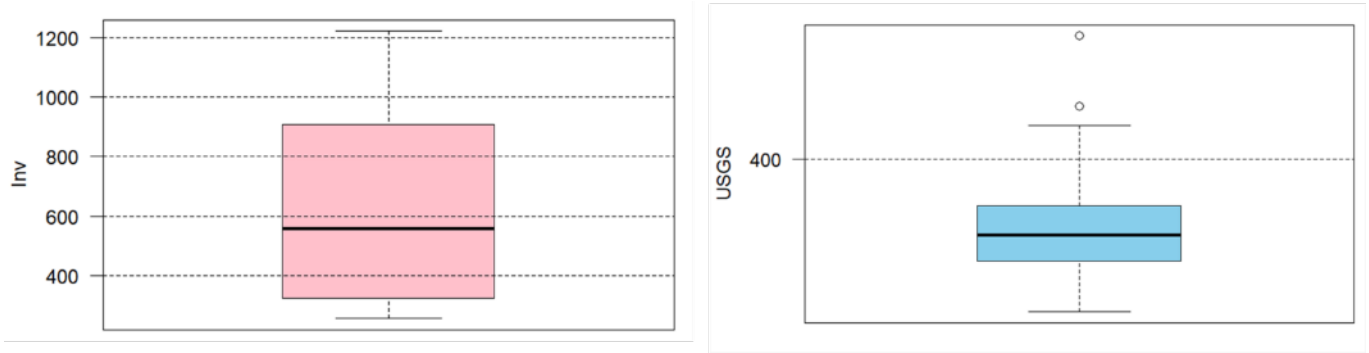


Figure 8. Boxplot comparison of V_{s30} values derived from two approaches. (a) V_{s30} values obtained from HVSR inversion. (b) V_{s30} values obtained from the USGS V_{s30} model.

Several studies have shown that the relationship between topographic slope and V_{s30} is not universally consistent when applied to regions with geological settings that differ from those used in the development of the original empirical models. Variations in lithology, degrees of rock weathering, and subsurface structural complexity can cause field-based V_{s30} values to deviate substantially from estimates derived solely from surface slope metrics (Allen and Wald, 2007; 2009). In the context of Ketahun, HVSR inversion results, which directly reflect local seismic response, exhibit a wider range of V_{s30} values and comparatively higher velocities in hilly areas. These patterns suggest the presence of relatively shallow bedrock that is not fully captured by slope-based proxy models.

Accordingly, the observed statistical differences do not merely reflect measurement inaccuracies but rather highlight fundamental distinctions between approaches based on local seismic response and those relying on surface morphological proxies. These findings emphasize that global topography-based V_{s30} models should be applied with caution in regions characterized by high geological heterogeneity, such as Ketahun.

4 CONCLUSION

This study sought to obtain a more representative estimation of V_{s30} in the Ketahun region through HVSR analysis combined with Monte Carlo inversion and to evaluate the results against the USGS topographic-slope-based model. The results reveal pronounced spatial variability in site conditions, with coastal areas characterized by low V_{s30} values associated with thick, soft sedimentary deposits, whereas the eastern and northern hilly sectors exhibit higher V_{s30} values indicative of shallower bedrock and stiffer subsurface materials. In comparison, the USGS model yields a narrower range of V_{s30} values and systematically underestimates site stiffness in hilly areas relative to the HVSR-based estimates. Statistical testing confirms that the differences between the two approaches are significant, suggesting that slope-based proxies may not adequately capture subsurface heterogeneity in geologically complex regions. These findings underscore the importance of site-specific geophysical measurements for seismic microzonation in Ketahun. Nevertheless, it must be acknowledged that HVSR inversion is inherently non-unique and that, in the absence of independent constraints such as borehole data or surface-wave dispersion measurements, the derived velocity models should be interpreted with appropriate caution. Future integration with complementary methods, such as Multichannel Analysis of Surface Waves (MASW) or borehole investigations, is therefore necessary to further reduce uncertainty and enhance the reliability of subsurface characterization.

DISCLAIMER

The authors declare no conflict of interest.

ACKNOWLEDGMENTS

The authors gratefully acknowledge the Geophysics Laboratory of the University of Bengkulu for providing access to the microtremor equipment used in the data acquisition. Appreciation is extended to the academic supervisors for their guidance throughout the development of this research, as well as to senior colleagues for their assistance during both data acquisition and manuscript preparation. The authors also acknowledge the United States Geological Survey (USGS) for supplying the V_{s30} dataset used as a comparative reference in this study.

REFERENCES

S. Akter. Seismic ground response analysis of input earthquake motion and site amplification factor at KUET. *Journal of the Civil Engineering Forum*, 8(1):45–54, 2022. doi:10.22146/jcef.3600.

T. I. Allen and D. Wald. Topographic slope as a proxy for seismic site-conditions (VS_{30}) and amplification around the globe. *USGS Open-File Report*, pages 1–70, 2007. doi:10.1785/0120060267.

T. I. Allen and D. Wald. On the use of high-resolution topographic data as a proxy for seismic site conditions (VS_{30}). *Bulletin of the Seismological Society of America*, 99(2A):935–943, 2009. doi:10.1785/0120080255.

S. Bonnefoy-Claudet, F. Cotton, and P.-Y. Bard. The nature of noise wavefield and its applications for site effects studies: A literature review. *Earth-Science Reviews*, 79:205–227, 2006. doi:10.1016/j.earscirev.2006.07.004.

S. Castellaro and F. Mulargia. Estimates of VS_{30} based on constrained H/V ratio measurements alone. In *Earthquake Hazard Evaluation*, pages 85–97. 2009. doi:10.1007/978-1-4020-9196-4_7.

A. Fatimah, S. P. D. Sriyanto, B. Sunardi, and W. Wandono. Identifikasi karakteristik tanah dan struktur kecepatan gelombang geser menggunakan data mikrotremor di daerah lembang, jawa barat. *Jurnal Geofisika*, 20(1):38, 2022. doi:10.36435/jgf.v20i1.521.

S. Foti, F. Hollender, F. Garofalo, D. Albarello, M. Asten, P.-Y. Bard, C. Comina, C. Cornou, B. Cox, G. D. Giulio, T. Forbriger, K. Hayashi, E. Lunedei, A. Martin, D. Mercerat, M. Ohrnberger, V. Poggi, F. Renalier, D. Sicilia, and V. Socco. Guidelines for the good practice of surface wave

analysis: a product of the interpacific project. *Bulletin of Earthquake Engineering*, 16:2367–2420, 2018. doi:10.1007/s10518-017-0206-7.

A. García-Jerez, J. Piña-Flores, F. J. Sánchez-Sesma, F. Luzón, and M. Perton. A computer code for forward calculation and inversion of the H/V spectral ratio under the diffuse field assumption. *Computers & Geosciences*, 97:67–78, 2016. doi:10.1016/j.cageo.2016.06.016.

A. I. Hadi, E. Suparka, S. Syuhada, A. Pramudita, and R. Yuniarto. Mapping landslide vulnerability using subsurface rock elastic parameters: A case study of lebong regency, bengkulu. *Kuwait Journal of Science*, 52 (2):100393, 2025. doi:10.1016/j.kjs.2025.100393.

B. Harlianto, D. I. Fadli, E. Sumanjaya, A. I. Hadi, A. Maulidiyah, S. Suwarsono, and E. H. Purwanto. Seismic vulnerability along the kaur–south oku highway in bengkulu, indonesia: planning for more resilient and safer cities. *Indian Geotechnical Journal*, pages 1–16, 2024. doi:10.1007/s40098-024-01101-6.

S. Hasaniyah, M. Arsyad, and A. Susanto. Evaluation of shear wave velocity using microtremor data at rammang-rammang maros karst area tn babul. *Jurnal Ilmu Fisika*, 17(2):171–181, 2025. doi:10.25077/jif.17.2.171-181.2025.

D. Heath, D. Wald, B. Worden, E. Thompson, and G. Smoczyk. A global hybrid VS_{30} map with a topographic slope-based default and regional map insets. *Earthquake Spectra*, 36(1):99–124, 2020. doi:10.1177/8755293020911137.

N. Hurukawa, B. R. Wulandari, and M. Kasahara. Earthquake history of the sumatran fault, indonesia, since 1892, derived from relocation of large earthquakes. *Bulletin of the Seismological Society of America*, 104 (4):1750–1762, 2014. doi:10.1785/0120130201.

G. Kencoro, I. Fatimah, S. Arifin, and S. Syuhada. Analisis zona rawan gempa bumi di kabupaten bengkulu selatan berdasarkan percepatan tanah puncak menggunakan formula kanai. *Jurnal Kumparan Fisika*, 6(2):75–82, 2023. doi:10.33369/jkf.6.2.75-82.

J. Lin, S. Moon, A. Yong, L. Meng, and P. Davies. Length-scale-dependent relationships between VS_{30} and topographic slopes in southern california. *Bulletin of the Seismological Society of America*, 109(6): 2614–2625, 2019. doi:10.1785/012019007.

A. M. Lubis, A. T. Siregar, D. Handayani, E. Maulana, and A. Prasetyo. Present-day inter-seismic velocities and fault slip rate of ketahun segment, sumatran fault system (sfs) inferred from global positioning system (gps) observations. *Tectonophysics*, 914:230879, 2025. doi:10.1016/j.tecto.2025.230879.

L. Z. Mase, N. Sugianto, and R. Refrizon. Seismic hazard microzonation of bengkulu city, indonesia. *Geoenvironmental Disasters*, 8(1), 2021. doi:10.1186/s40677-021-00178-y.

N. Metropolis, A. Rosenbluth, M. Rosenbluth, A. Teller, and E. Teller. Equation of state calculations by fast computing machines. *Journal of Chemical Physics*, 21(6):1087–1092, 1953. doi:10.1063/1.1699114.

R. Myers and A. Aydin. The evolution of faults formed by shearing across joint zones in sandstone. *Journal of Structural Geology*, 26(5): 947–966, 2004. doi:10.1016/j.jsg.2003.07.008.

A. S. Nugraheni, A. Setianto, and H. Setiawan. Comparison of VS_{30} value from microtremor data based on spt drill test of young merapi deposits in opak river, yogyakarta. *Jurnal Geosains dan Remote Sensing*, 5 (2):101–110, 2024. doi:10.23960/jgrs.ft.unila.304.

S. Parolai, P. Bormann, and C. Milkereit. New relationships between VS, thickness of sediments and resonance frequency calculated by the H/V ratio of seismic noise for the cologne area (germany). *Bulletin of the Seismological Society of America*, 92(6):2521–2527, 2002. doi:10.1785/0120010248.

K. Sieh and D. Natawidjaja. Neotectonics of the sumatran fault, indonesia. *Journal of Geophysical Research: Solid Earth*, 105(B12):28295–28326, 2000. doi:10.1029/2000jb900120.

A. V. H. Simanjuntak, R. A. Putra, H. Suryadi, B. Rambe, and R. Hidayat. Analisis kerentanan seismik dan model VS_{30} berdasarkan survei mikrotremor HVSR dan SPAC (studi kasus: Kota banda aceh). *Jurnal Lingkungan dan Bencana Geologi*, 12(2):125, 2021. doi:10.34126/jlbg.v12i2.324.

W. Stephenson. HVSR, SSR, and VS_{30} values at three new zealand basin arrays. *Journal of Earthquake Engineering*, 11(6):987–1009, 2007. doi:10.1080/13632460701385358.

A. Susilo, A. Prasetyo, G. Wijaya, R. Hidayat, and R. Nurcahyo. Seismic site characterization of malang regency (indonesia) using HVSR inversion. *Kuwait Journal of Science*, 53(1):100486, 2024. doi:10.1016/j.kjs.2025.100486.

M. Wathelet, J.-L. Chatelain, C. Cornou, G. D. Giulio, B. Guillier, M. Ohrnberger, and A. Savvaidis. Geopsy: A user-friendly open-source tool set for ambient vibration processing. *Seismological Research Letters*, 91(3):1878–1889, 2020. doi:10.1785/0220190360.

A. Zaenudin, A. Farduwin, G. I. B. Darmawan, and K. Karyanto. Shear wave velocity model using HVSR inversion beneath bandar lampung city. *Earthquake Science*, 37(4):337–351, 2024. doi:10.1016/j.eqs.2024.04.004.